Surface Reconstruction of the Lamellar Morphology in a Symmetric Poly(styrene-*block*-butadiene-*block*-methyl methacrylate) Triblock Copolymer: A Tapping Mode Scanning Force Microscope Study

Wolfgang Stocker,*,† Jörg Beckmann,‡,§ Reimund Stadler,‡ and Jürgen P. Rabe†

Institut für Physik, Physik von Makromolekülen, Humboldt Universität zu Berlin, Invalidenstrasse 110, D-10115 Berlin, Germany, and Institut für Organische Chemie, Johannes Gutenberg Universität Mainz, J. J. Becherweg 18-20, D-55099 Mainz, Germany

Received March 14, 1996; Revised Manuscript Received August 3, 1996[⊗]

ABSTRACT: The surface morphology of a symmetric poly(styrene-*block*-butadiene-*block*-methyl methacrylate) triblock copolymer (PS-*b*-PB-*b*-PMMA) with 6 wt % PB has been investigated by tapping mode scanning force microscopy (SFM). The results are compared to the bulk morphology as determined by transmission electron microscopy (TEM). In solvent-cast films PS/PMMA lamellae are formed, which are oriented nearly perpendicular to the free surface. Like in the bulk, also at the free film surface polybutadiene spheres are located at the lamellar PS/PMMA interface. However, contrary to the bulk, the surface morphology includes a large number of defects such as curved lamellar and disclinations, and the lamellar long period is doubled, from 42.7 ± 0.5 nm in the bulk to 85 ± 5 nm at the free surface, indicating a surface reconstruction. The double spacing can be explained by a surface buckling in registry with the underlying PS/PMMA lamellae. The composition of the outermost surface layer is discussed.

Introduction

The microphase separation of symmetrical poly(A-*block*-B-*block*-C) triblock copolymers consisting of three blocks of different chemical nature can result in ordered microdomain morphologies.[1−5] Examples include poly(styrene-*b*-butadiene-*b*-methyl methacrylate) triblock copolymers (PS-*b*-PB-*b*-PMMA), in which the morphology is governed by the relatively weak incompatibility of the end blocks PS and PMMA in comparison to the strong incompatibility with the polybutadiene midblock.[2−5] As a result of the phase separation, these multicomponent systems form self-assembled ordered structures with periodicities on the nanometer scale.

While the experimental work on block copolymers deals mainly with the bulk morphology, only a limited amount of information is available on the structure and orientation of microdomains near the free surface. The resolution achieved by scanning force microscopy (SFM)[6−12] renders it a valuable tool to investigate the morphology and molecular packing of polymers at free surfaces and interfaces.[13−24] The high lateral resolution down to the atomic and molecular scale offered by SFM and its applicability to native samples without modifications or staining are ideal features for morphological studies on block copolymers. Operation of the SFM in the so-called tapping mode[11] (vertical oscillation of the cantilever) enables one to minimize lateral forces and to investigate soft surfaces without plastic deformation.

This paper describes the surface morphology of a poly(styrene-*block*-butadiene-*block*-methyl methacrylate) triblock copolymer (SBM6), which is nearly symmetric with respect to the PS and PMMA blocks with a short center block of about 6 wt % PB. The surface morphology of SBM6 is analyzed by SFM and compared to the bulk morphology as determined by TEM for the same sample.

Table 1. Characteristics of the Components in the Triblock Copolymer SBM6[a]

	PS	PB	PMMA
w	0.45	0.06	0.49
ϕ	0.47	0.075	0.455
γ/mN m^{-1}	40.7	30−32	41.1

[a] w = weight fraction; ϕ = volume fraction; γ = surface tension (polymer/air) at 20 °C (from refs 28−30).

In triblock copolymers such as SBM6, the elastomer midblock PB is tightly connected between the two glasslike end blocks PS and PMMA. Therefore, the PB block cannot undergo large scale phase separation. The bulk morphology of SBM6 was established by transmission electron microscopy (TEM).[3,5] As deduced from TEM, SBM6 forms a "ball at the wall" structure,[3] in which PB spheres are located at the lamellar PS/PMMA interface. Our SFM results on SBM6 show a clear discrimination between the surface and bulk nanostructures. The surface structure of SBM6 exhibits a reconstructed morphology, in which the overall lamellar long period is twice the bulk lamellar long period. The surface free energy is the driving force that stabilizes the reconstructed morphology near the free surface.

Experimental Section

Materials. Synthesis and characterization of the poly(styrene-*block*-butadiene-*block*-methyl methacrylate) triblock copolymer (SBM6) is described elsewhere.[2,3] It has a molecular weight of 225 000 with a polydispersity of 1.11. Further characteristics are given in Table 1.

Sample Preparation. Films of poly(styrene-*b*-butadiene-*b*-methyl methacrylate) with a thickness in the range of 10−20 μm were cast from chloroform solution (10% w/v) on glass cover slides by slowly evaporating the solvent at 25 °C over a

* To whom correspondence should be addressed.
† Humboldt Universität zu Berlin.
‡ Johannes Gutenberg Universität Mainz.
§ Present address: Institut für Theoretische und Physikalische Chemie, Universität Potsdam, Kantrasse 55, D-14513 Teltow, Germany.
⊗ Abstract published in *Advance ACS Abstracts,* October 1, 1996.

S0024-9297(96)00400-7 CCC: $12.00

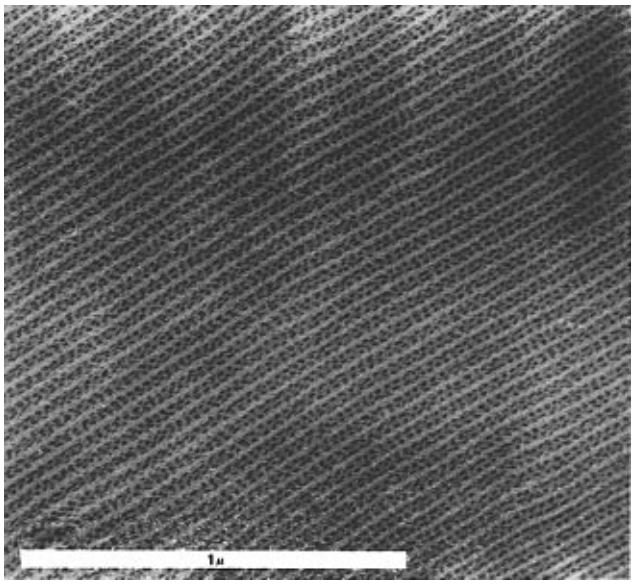

Figure 1. Transmission electron micrograph of the triblock copolymer SBM6 using OsO_4 as the staining agent. The system forms a lamellar morphology. The polybutadiene (PB) spheres are strongly stained and appear dark in TEM, while the PS lamellae (gray) only show a weak contrast with respect to the PMMA lamellae (bright). Polybutadiene spheres are located at the PS/PMMA interface (ls morphology). The long period of the lamellar structure is 42.7 ± 0.5 nm. The estimated diameter of the PB spheres is around 9 nm. The PB spheres show a deeper penetration into the PS phase. Only one main lamellar orientation is present in the observed area (1.7 × 1.7 μm^2).

period of 1 week. For further equilibration, the transparent films were dried at reduced pressure (10^{-2} mbar) for 24 h at 100 °C. For SFM analysis, no staining or sectioning was necessary, contrary to the preparation for TEM.

Scanning Force Microscopy (SFM). SFM experiments were carried out with a Nanoscope III (Digital Instruments, Inc., Santa Barbara, CA) in the tapping mode, where the change of the vertical cantilever oscillation amplitude is detected, which is caused by touching the sample surface periodically. In tapping mode operation, lateral shear forces are minimized. Silicon cantilevers (length 125 μm, width 30 μm, thickness 3−5 μm) with a spring constant between 17 and 64 N/m and a resonance frequency in the range of 240−400 kHz were used. Resonance peaks in the frequency response of the cantilever, typically in the range between 280 and 320 kHz, were chosen for the tapping mode oscillation. Vibration amplitudes usually in the range between 20 and 30 nm were applied. The SFM images were obtained with an E-type scan head (maximum scan range 12 × 12 μm^2). The amplitude of the oscillation was calibrated with respect to the vertical position of the piezoelectric scanner. Imaging was performed by displaying the amplitude signal (incoming signal for the feedback system) and the height signal (output of the feedback system). Feedback parameters were optimized by minimizing changes in the amplitude signal. All images presented are height images. Scanning frequencies were usually in the range between 0.4 and 2 Hz per line. The measurements were carried out in air under normal conditions. For distance calibration of the piezo controller, images of gold calibration gratings were employed.

Transmission Electron Microscopy (TEM). TEM was performed on a Philips transmission electron microscope operating at 80 kV. Ultrathin sections of the block copolymer were obtained using a Reichert Ultramicrotome equipped with a diamond knife. The ultrathin sections were mounted on gold grids and stained with OsO_4 vapor for TEM analysis.

Results

In the following section, the morphology of SBM6 obtained by SFM will be compared to the corresponding

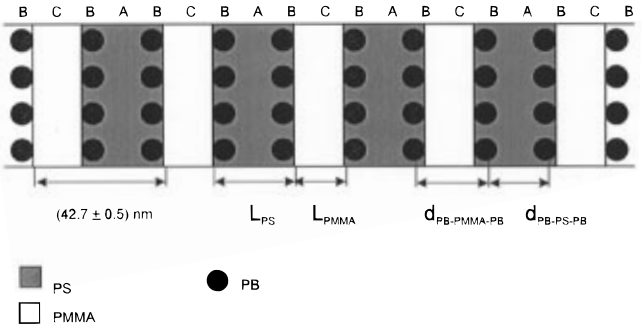

Figure 2. Schematic representation of the bulk morphology of SBM6 as determined from transmission electron microscopy. The thicknesses of corresponding PS and PMMA lamellae are $L_{PS} = 26 \pm 5$ nm and $L_{PMMA} = 17 \pm 5$ nm, respectively. PB spheres are located at the phase boundaries between PS/PMMA. Note that the PB spheres show a deeper penetration into the PS phase. This results in a morphology in which the PB spheres are separated by two alternating periodicities of $d_{PB-PS-PB} = 18 \pm 3$ nm and $d_{PB-PMMA-PB} = 24 \pm 4$ nm.

Table 2. Interaction parameters χ_{AB} between the Components in P(S-*b*-B-*b*-MMA)[5]

polymer pair	PS/PMMA	PS/PB	PMMA/PB
χ_{AB}	0.03	0.045	0.071

TEM results. The differences between surface and bulk morphology will be discussed.

1. Transmission Electron Microscopy: Bulk Morphology of SBM6. Figure 1 shows a transmission electron micrograph of SBM6 using OsO_4 as the staining agent. The system exhibits a lamellar morphology as described before.[5] Using OsO_4 as the staining agent, the polybutadiene blocks are strongly stained and appear dark in TEM, while the PS lamellae (gray) only show a weak contrast with respect to the PMMA lamellae (bright). The system forms homogeneously ordered lamellae over more than 1.5 × 1.5 μm^2. Only one main lamellar orientation is present in Figure 1 (from lower left to upper right). The PB blocks (dark) are located at the phase boundary between the PS (gray lamellae) and the PMMA (bright lamellae). The TEM micrograph provides the basic information needed for a complete structural characterization of the bulk structure, as presented schematically in Figure 2. A quantitative analysis beyond the published work[5] gives the following results: (i) The overall lamellar long period is 42.7 ± 0.5 nm. (ii) From the quantitative analysis of the electron micrograph, the individual thicknesses of the corresponding PS and PMMA lamellae are 26 ± 5 nm and 17 ± 5 nm, respectively. (iii) The PB spheres, which are located at the phase boundary between PS and PMMA lamellae, *penetrate deeper into the PS phase.* The result is a morphology in which the PB spheres are separated by two alternating periodicities of $d_{PB-PS-PB} = 18 \pm 3$ nm and $d_{PB-PMMA-PB} = 24 \pm 4$ nm. The estimated size of the PB particles is about 9 nm.

The deeper penetration of the PB particles into the PS phase (as schematically shown in Figure 2) can be explained by the different interaction parameters between the PS/PB and the PB/PMMA pairs, respectively. Large positive interaction parameters (strong incompatibility) lead to high interfacial tensions.[25−27] Three interaction parameters must be taken into account for the triblock copolymer SBM6 (Table 2). Since the interfacial tension between PS and PB is much smaller than that between PB and PMMA, PB reduces its interfacial energy by penetrating into the PS lamellae.

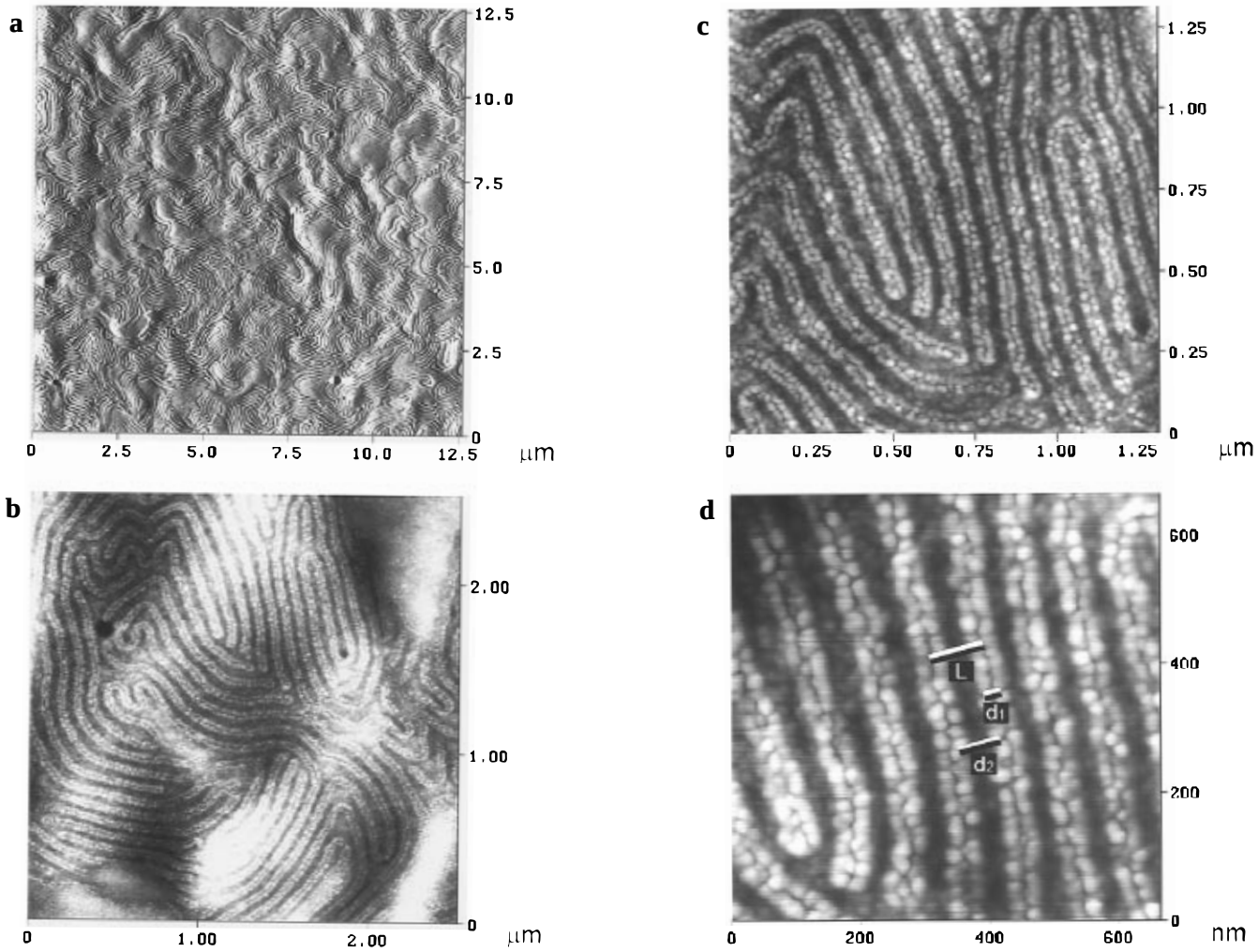

Figure 3. Scanning force microscopy (SFM) images of solution cast films of the triblock copolymer SBM6 (height imaging, no filter, no staining). (a) Lamellar morphology over an area of 12 × 12 μm^2 (*z* scale 9 nm). The lamellae are oriented mainly perpendicular to the observed surface. In comparison to the highly ordered bulk morphology (Figure 1), the surface morphology shows a large number of defects such as lamellar bends and disclinations. (b) Lamellar morphology over an area of 2.5 × 2.5 μm^2 (*z* scale 9 nm), showing PS/PMMA lamellae with polybutadiene spheroids located at the PS/PMMA interface. The estimated diameter of PB microdomains is about 14 nm. Only small areas, in which the lamellae are oriented parallel to the observed surface are visible (upper and lower right). In these areas, the polybutadiene blocks can be recognized as small spheroids on top of the lamellar surface. (c) 1.3 × 1.3 μm^2 area, showing the lamellar spherical morphology (*z* scale 7 nm). Comparison with the bulk morphology (Figures 1 and 2) shows that the surface morphology observed by SFM shows a long period, which is doubled from 42.7 ± 0.5 nm in the bulk to 85 ± 5 nm at the surface. The result is a *missing row surface reconstruction* of the lamellar morphology. (d) High magnification SFM image (700 × 700 nm^2, *z* scale 7 nm) of the *missing row reconstruction* of SBM6. The overall lamellar long period is $L = 85 \pm 5$ nm. The PB spheroids, indicating the phase boundary between PS and PMMA, are separated by *two alternating lamellar widths* of $d_1 = 22 \pm 5$ nm and $d_2 = 63 \pm 5$ nm. The smaller lamellae observed on the surface may be attributed to the PMMA phase, as explained in Figure 4.

The result is a morphology in which the PB spheres are separated by two alternating periodicities, $d_{PB-PS-PB}$ and $d_{PB-PMMA-PB}$ (Figure 2). Since the polybutadiene domains most likely have a spherical or ellipsoidal shape, the morphology is described as *lamellar-spherical* (ls) structure.[5]

2. Scanning Force Microscopy: Surface Reconstruction of the Bulk Morphology. Scanning force microscopy was performed on solvent-cast films without staining. SFM images of SBM6 are displayed in Figure 3a−d. Figure 3a reveals a lamellar surface morphology. Comparison with the bulk morphology shows a somewhat larger number of defects such as curved lamellae and disclinations at the free surface. However, it must be noted that Figure 1a displays a particularly well-ordered region (see for comparison also images in ref 5). At higher magnification (Figure 3b), spheroids located at the lamellar interfaces are clearly seen. Areas in which spheroids cover the surface completely are very small (upper and lower right in Figure 3b).

Even higher magnification SFM images of SBM6 are shown in Figure 3c,d. From a series of experiments the following dimensions of the surface morphology are obtained: (i) The overall lamellar long period perpendicular to the lamellae is $L = 85 \pm 5$ nm (as indicated in Figure 3d). (ii) The spheroid particles are separated by two alternating periodicities (Figure 3d) of $d_1 = 22 \pm 5$ nm and $d_2 = 63 \pm 5$ nm. The average diameter of the spheroids is about 14 nm.

Comparison with the results obtained from TEM shows that *the overall lamellar long period at the surface is twice the bulk value.*

Since the long period at the surface is an integer multiple of the bulk value, we attribute this result to a "surface reconstruction" of the lamellar morphology, in analogy to the surface reconstruction observed for metallic or semiconducting crystals. The reconstruction

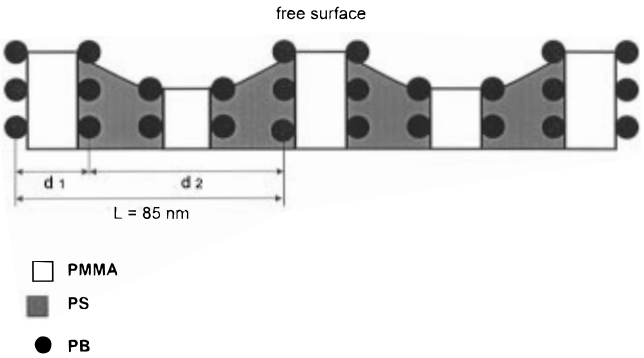

Figure 4. Schematic representation of the *surface reconstructed morphology* of the triblock copolymer SBM6 (cross sectional model, side view). The vertical shift of neighboring lamellae leads to a characteristic surface profile. This results in a "buckling" of the polymer film at the free surface. The outermost lamellae (unshaded) are pronounced in SFM. The resulting periodicity at the surface of 85 ± 5 nm is twice the bulk lamellar long period (missing row reconstruction).

can be described by a surface "buckling" of the polymer film. A schematic representation of the *missing row reconstruction* is shown in Figure 4 (cross sectional model). Since the lamellae are oriented perpendicular to the free surface, a vertical shift of alternating lamellae would explain the periodicity of twice the bulk lamellar long period, where the outermost lamellae (Figure 4) appear pronounced in the images.

Discussion

1. Attribution to Blocks. In analogy to the bulk morphology we attribute the spheroids in the SFM images to PB at the interface between lamellae composed of PS and PMMA. In the SFM, the PB spheres appear bright, while the PS and PMMA lamellae appear dark. *The SFM images do not differentiate between lamellae of PS and PMMA* (Figure 3b−d). In the present communication the individual lamellar thicknesses of PS and PMMA have been analyzed from SFM data by *measuring the distances between the rows of PB spheroids.* Since the PB is arranged *at the lamellar PS/PMMA interfaces*, the lamellar structure is observed. The small PB midblocks act as a marker, indicating the phase boundaries between the PS and PMMA lamellae. The spheroids are separated by *two alternating periodicities* of d_1 and d_2 (Figure 3d and Figure 4), resulting in an overall lamellar long period of L.

The buckling means that the total free surface area is increased. The model shown in Figure 4 indicates that this is due to the free surface of the shaded lamellae. Since the surface tension of PS is smaller than that of PMMA (Table 1), one may attribute the shaded lamellae to PS and the unshaded to PMMA. The results are in agreement with the experimentally obtained lamellar widths by TEM and SFM.

2. Size of Spherical PB Domains. In the SFM images the PB particles appear as deformed spheres with an average diameter of about 14 nm. Due to their low surface energy, they tend to increase their free surface contact area. Therefore the spheres may be flattened on the free surface, which would explain their somewhat enlarged diameter as compared to TEM (14 nm vs 9 nm). In addition one has to consider the imaging process with the SFM. It can be described as a "convolution" of the specimen topography with the actual tip shape (the term "convolution" is here not meant in its strict mathematical sense).[9] In order to deconvolute the sample shape one would need a precise description of the tip. Since this is very difficult, we only note that the finite tip radius enlarges generally the diameter of a protrusion on the surface.

3. Film Formation and Orientation of Lamellae Relative to the Free Surface. Preparation of copolymer films by solvent evaporation does not necessarily produce an equilibrium morphology. For diblock copolymers it has been shown that the rate of solvent evaporation during sample preparation affects the surface composition.[30] If the solvent evaporation is fast, one finds that the structure is kinetically controlled and a nonequilibrium structure is frozen in. If the evaporation rate is slow, then the system can more closely approach its equilibrium structure. This is consistent with the findings in this study, where the equilibrium morphology of SBM6 was obtained by allowing the solvent to evaporate slowly within 1 week. At very high evaporation rates (e.g. in spin-coated films), no oriented lamellar structures were obtained.

The observed surface structure, where the PS/PMMA lamellae are oriented perpendicular to the free surface can be explained by the process during film formation. The surface energies of the three components are slightly different (Table 1). The lowest surface free energy block PB tends to create a free surface contact. As found by SFM, PB spheres always occupy the free surface. Since the PB blocks are tightly connected between the PS and PMMA end blocks, they cannot undergo large scale phase separation. Then, during film formation, both end blocks PS and PMMA are drawn to the free surface. The result is a structure, where all three components are present near the polymer/air interface. In our case it is a sequence of alternating PS and PMMA lamellae perpendicular to the free surface.

When casting the film from solution, we are concerned with the onset of a phase separation from a homogeneous solution. It is known for AB-diblock copolymers[29,31,32] that, during film casting, the surface layer is formed first and if ordered structures are created, they grow from the interface. Selective solvents do cause surface enrichment of the most soluble species. Analysis of the Hildebrand solubility parameter δ values reported in the literature[33] indicate that chloroform is a mutual solvent for PS and PMMA, but it is more selective toward PB (19 ± 1, 18.9 ± 0.5, 17.1 ± 0.5, and 19.0 ± 0.1 $MPa^{1/2}$ for PS, PMMA, PB, and chloroform, respectively). These parameters describe the enthalpy of mixing of the three polymer/solvent pairs. In general, $(\delta_{polymer} - \delta_{solvent})^2$ must be small for the polymer to be soluble. The PB midblock is slightly less soluble in chloroform than the PS and PMMA components. Thus it is likely that during film casting the tendency of the PB component to occupy the film/air interface is counteracted by the higher affinity of the PS and PMMA block chains for the solvent. In the present case, neither of these two effects dominates, since all three phases are present at the free surface.

4. Composition of the Outermost Surface Layer and Compatibility of Polystyrene and Poly(methyl methacrylate) near the Free Surface. Alternatively to the structure model in Figure 4, in which all three phases are located *separately* at the free surface, one may suppose that the lowest surface free energy block (PB) forms a thin, continuous surface layer, which is supported by the underlying PS/PMMA lamellae. This model may be motivated by diblock studies. TEM studies of poly(styrene-*b*-butadiene) diblock copolymers, which exhibit varying morphologies, lead to the conclu-

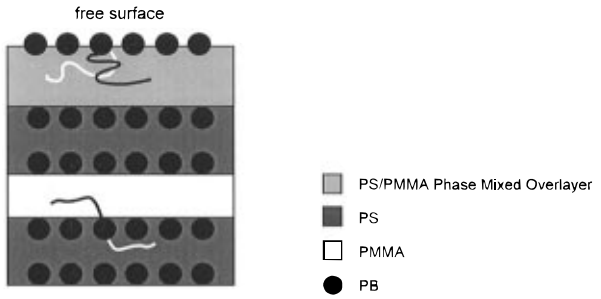

Figure 5. Schematic model of the morphology of SBM6 as found in the upper und lower right regions of Figure 3b. In these regions, the PS/PMMA lamellae are oriented *parallel* to the free surface. Since the PB spheres always occupy the polymer/air interface, the PS and PMMA end blocks are forced to become miscible in the near surface region. A phase-mixed PS/PMMA overlayer is formed. PS and PMMA molecules are drawn schematically in the figure.

sion that the block chains with lower surface tension always cover the free surface.[29,34] TEM of cross sections, which include the surface and near surface region of a PS/PB diblock copolymer, demonstrates the connection between the surface and bulk morphology. The lowest surface energy block PB wets the surface completely. As found for PS/PB diblock copolymers, the thickness of this overlayer is approximately half of the average thickness of the PB lamellae.[35] In the case of the triblock copolymer SBM6, the situation is quite different. The PB midblock is tightly connected between the end blocks PS and PMMA and cannot undergo large scale phase separation. Since the volume fraction of the PB midblock is about 7.5%, the PB block chains cannot cover the free surface completely. The result is the morphology described in Figure 4.

A series of experiments shows that small surface areas exist in which the spheroids cover the surface completely (upper and lower right in Figure 3b). In these areas, the PB spheroids can be recognized as small spheroids. These surface areas are attributed to lamellae, which are oriented parallel to the observed surface. This structure may be supported by underlying PS/PMMA lamellae, *which are oriented parallel to the free surface*. In this case, the low surface energy of the PB component would induce a miscibility of the two glass blocks PS and PMMA, which are weakly incompatible in comparison to the PS/PB and PB/PMMA pairs, respectively. A structural model of the resulting morphology at the film surface is given in Figure 5. Since the lamellae are aligned *parallel to the free surface* and the PB midblocks occupy the polymer/air interface, *a phase-mixed overlayer is formed*. In this case it is the minimization of the surface free energy which leads to a thin outermost PB layer and the PS and PMMA blocks are forced to become miscible in the near surface region. This phase-mixed overlayer is consistent with the results reported for thin films of PS-*b*-PMMA diblock copolymers.[35]

5. Surface Topography and Contrast Mechanism in Tapping Mode Scanning Force Microscopy. The interaction of a forced cantilever oscillation with a specimen in tapping mode scanning force microscopy depends on the viscoelastic behavior of the polymer. In order to obtain topographical information, the tip must interact with the surface. The frequency of the cantilever oscillation must be high enough to exclude a viscous contribution to the deformation of the polymer.

Having examined the topography at the surface of a multicomponent system, we now turn attention to the details of the time and frequency dependence of the viscoelastic functions (storage modulus $G'(\omega)$ and loss modulus $G''(\omega)$) of the components. As shown by the results (Figure 3) a good contrast is observed between the elastomer PB and the two glasslike blocks PS and PMMA, respectively. However, this contrast observed between the rubber- and glasslike blocks cannot be easily explained with their different viscoelastic properties. For comparison of two polymers (i.e. PS and PB), two quantities are conventionally selected as gauges of the location of the glass transition on the frequency scale: the frequency where $G' = 10^8$ dyn/cm^2 (an intermediate value between the typical values for the rubberlike and the glasslike states) and the frequency where the loss tangent has a maximum. The frequency, which characterizes the glass transition zone for 1,2-polybutadiene is around 10 kHz ($\log \nu_0 = 3.8$).[36] In the presented tapping mode SFM images obtained around 300 kHz, a good contrast between the rubberlike PB and the glasslike components PS and PMMA was observed. This frequency is 1 order of magnitude above the glass transition zone for PB. Thus it is unlikely that the contrast between the glass- and rubberlike blocks is due to a different plastic deformation. For PB and PS or PMMA the measured contrast is therefore mainly caused by topographical features on the surface, which are attributed to the different interfacial energies of the components at the polymer/air interface. The measured contrast is attributed to a real height profile, which is modulated by the underlying lamellae, spheres, etc. Further lowering the cantilever oscillation frequency (below 10 kHz) and increasing the oscillation amplitude would allow one to estimate the local viscoelastic behavior of different components at the surface.

Conclusion

Tapping mode scanning force microscopy reveals detailed structural information on block copolymer surfaces. In a triblock copolymer system, the formation of lamellae oriented normal to the surface has been observed for the first time. A mechanism of film formation during solution casting has been discussed. We conclude that the morphology in the near surface region differs from that observed in bulk in the sense of a surface reconstruction (surface buckling).

The measured contrast in tapping mode SFM has been explained by topographical features on the surface, which are caused by the different interfacial energies of the components at the polymer/air interface. Future work should help to describe further important surface-related properties such as adhesion, wettability, and local viscoelastic properties of the components in the vicinity of free surfaces.

Acknowledgment. This work has been supported by the ESPRIT Long Term Research Project PRONANO 8523. The authors are indebted to Dr. Clemens Auschra (Institut für Organische Chemie, Mainz) for synthesis. Special thanks to Dr. Britta L. Schürmann and Dr. Frank Schabert for reading and discussing the manuscript.

References and Notes

(1) Riess, G. In *Thermoplastic Elastomers. A Comprehensive Review*; Ledge, N. R., Holden, G., Schroeder, H. E., Eds.; Hanser: Munich, 1987.

(2) Auschra, C.; Stadler, R. *Macromolecules* **1993**, *26*, 2171.
(3) Beckmann, J.; Auschra, C.; Stadler, R. *Makromol. Chem., Rapid. Commun.* **1994**, *15*, 67.
(4) Krappe, U.; Stadler, R.; Voigt-Martin, I. *Macromolecules* **1995**, *28*, 4558.
(5) Stadler, R.; Auschra, C.; Beckmann, J.; Krappe, U.; Voigt-Martin, I.; Leibler, L. *Macromolecules* **1995**, *28*, 3080.
(6) Binnig, G.; Quate, C. F.; Gerber, C. *Phys. Rev. Lett.* **1986**, *56*, 930.
(7) Hansma, P. K.; Elings, V.; Marti, O.; Braker, C. E. *Science* **1988**, *242*, 209.
(8) Drake, B.; Prater, C. B.; Weisenhorn, A. C.; Gould, S. A. C.; Albrecht, T. R.; Quate, C. F.; Cannel, P. S.; Hansma, H. G.; Hansma, P. K. *Science* **1989,** *243*, 5586.
(9) Butt, H.-J.; Guckenberger, R.; Rabe, J. P. *Ultramicroscopy* **1992**, *46*, 375.
(10) Ohnsorge, F.; Binnig, G. *Science* **1993**, *260*, 1451.
(11) Zhong, Q.; Inniss, D.; Elings, V. *Surf. Sci.* **1993**, *290*, 688.
(12) Spatz, J. P.; Sheiko, S.; Möller, M.; Winkler, R. G.; Reinecker, P.; Marti, O. *Nanotechnology* **1995**, *6*, 40.
(13) Lotz, B.; Wittmann, J. C.; Stocker, W.; Magonov, S. N.; Cantow, H.-J. *Polym. Bull.* **1991**, *26*, 209.
(14) Annis, B. K.; Schwark, D. W.; Reffner, J. R.; Thomas, E. L.; Wunderlich, B. *Makromol. Chem.* **1992**, *190*, 258.
(15) Hansma, H. G.; Motademi, F.; Smith, P.; Hansma, P. K.; Wittmann, J. C. *Polymer* **1992**, *33*, 674.
(16) Dietz, P.; Hansma, P. K.; Ihn, K. J.; Motamedi, F.; Smith, P. *J. Mater. Sci.* **1993**, *28*, 1372.
(17) Snétivy, D.; Guillet, J. E.; Vansco, G. J. *Polymer* **1993**, *34*, 429.
(18) Juhué, D.; Lang, J. *Langmuir* **1993**, *9*, 792.
(19) Stocker, W.; Magonov, S. N.; Cantow, H.-J.; Wittmann, J. C.; Lotz, B. *Macromolecules* **1993**, *26*, 5915.
(20) Snetivy, D.; Guillet, J. E..; Vansco, G. J. *Polymer* **1994**, *35*, 461.
(21) Stocker, W.; Magonov, S. N.; Cantow, H.-J.; Wittmann, J. C.; Lotz, B. *Macromolecules* **1994**, *27*, 6690.
(22) Stocker, W.; Graff, S.; Lang, J.; Wittmann, J. C.; Lotz, B. *Macromolecules* **1994**, *27*, 6677.
(23) Stocker, W.; Schumacher, M.; Graff, S.; Lang, J.; Wittmann, J. C.; Lovinger, A. J.; Lotz, B. *Macromolecules* **1994**, *27*, 6948.
(24) van Dijk, M. A.; van den Berg, R. *Macromolecules* **1995**, *28*, 6773.
(25) Helfand, E. *Macromolecules* **1975**, *8*, 552.
(26) Helfand, E.; Wasserman, Z. R. *Macromolecules* **1976**, *9*, 879.
(27) Helfand, E.; Wasserman, Z. R. *Macromolecules* **1978**, *11*, 960.
(28) Wu, S. *J. Phys. Chem.* **1970**, *74*, 632.
(29) Turturro, A.; Gattigila, E.; Vacca, P.; Viola, G. T. *Polymer* **1995**, *21*, 3987.
(30) Green, P. F.; Christensen, T. M.; Russel, T. M.; Jérôme, R. *Macromolecules* **1989**, *22*, 2189.
(31) Fredrickson, G. H. *Macromolecules* **1987**, *20*, 2535.
(32) Green, P. F.; Christensen, T. M.; Russel, T. P. *Macromolecules* **1991**, *24*, 252.
(33) Grulke, E. A. In *Polymer Handbook*, 3rd ed.; Brandrup, J., Immergut, E. H., Eds.; Wiley: New York, 1989.
(34) Hasegava, H.; Hashimoto, T. *Polymer* **1992**, *33*, 475.
(35) Russel, T. P.; Menelle, A.; Anastasiadis, S. H.; Satija, S. K.; Majkrzak, C. F. *Macromolecules* **1991**, *24*, 6263.
(36) Ferry, J. D. *Viscoelastic Properties of Polymers*, 3rd ed.; John Wiley & Sons, Inc.: New York, 1980, p 324.

MA9604000